applied sciences

MDPI

Article

Short-Term Load Forecasting of the Greek Electricity System

George Stamatellos and Tassos Stamatelos *

Department of Mechanical Engineering, University of Thessaly, 383 34 Volos, Greece
* Correspondence: stam@uth.gr; Tel.: +30-2421-074-067

Featured Application: In spite of the significant developments in machine learning methods employed for short-term electrical load forecasting on a Country level, the complexity and diversity of the problem points to the need for investing more research effort in the selection of representative input datasets for the training. This is demonstrated in the example of the Greek electricity system, where careful selection and quality assurance of input data resulted in quite acceptable levels of prediction accuracy, even when training standard, robust feed-forward artificial neural networks.

Abstract: Short-term load forecasting is an essential instrument in power system planning, operation, and control. It is involved in the scheduling of capacity dispatch, system reliability analysis, and maintenance planning for turbines and generators. Despite the high level of development of advanced types of machine learning models in commercial codes and platforms, the prediction accuracy needs further improvement, especially in certain short, problematic time periods. To this end, this paper employs public domain electric load data and typical climatic data to make 24-hour-ahead hourly electricity load forecasts of the Greek system based on two types of robust, standard feed-forward artificial neural networks. The accuracy and stability of the prediction performance are measured by means of the modeling error values. The current prediction accuracy levels of mean absolute percentage error, mean value $\mu = 2.61\%$ with $\sigma = 0.33\%$ of the Greek system operator for 2022, attained with noon correction, are closely matched with a simple feed-forward artificial neural network, attaining mean value $\mu = 3.66\%$ with $\sigma = 0.30\%$ with true 24-hour-ahead prediction. Specific instances of prediction failure in cases of unexpectedly high or low energy demand are analyzed and discussed. The role of the structure and quality of input data of the training datasets is demonstrated to be the most critical factor in further increasing the accuracy and reliability of forecasting.

Keywords: electricity load curve; day-ahead forecasting; artificial neural networks

Citation: Stamatellos, G.; Stamatelos, T. Short-Term Load Forecasting of the Greek Electricity System. *Appl. Sci.* **2023**, *13*, 2719. https://doi.org/10.3390/app13042719

Academic Editors: Kuo-Ping Lin, Chien-Chih Wang and Chih-Hung Jen

Received: 3 February 2023
Revised: 16 February 2023
Accepted: 18 February 2023
Published: 20 February 2023

1. Introduction

The fundamental objective of electric power industry deregulation is to maximize efficient generation and consumption of electricity and reduce energy prices. To achieve these goals, accurate and efficient electricity load forecasting is becoming more and more important [1]. Distribution and transmission system operators are based on these forecasts in order to deal with the stochastic variations of the distributed renewable power sources connected to the grid [2]. This holds true both for the aggregate system load (i.e., on a country basis) as well as for the load met by micro-grids. Although the main body of the specialized literature addresses the prediction of the total load on a country, region, or county/community level, significant attention is shifted to the bus load of the transmission and distribution systems, which are more affected by the stochastic nature of individual loads [3]. Moreover, forecasting aggregate system load and electricity price has become a major issue in modern power systems, a pre-requisite for price forecasting [4]. Thus, short-term load forecasting (STLF) is an indispensable tool in power systems planning, maintenance, and management and in smart grid applications [5]. It counts decades of research activity and applications, with a multitude of forecasting models, methodologies, and tools for day-ahead and hour-ahead load predictions.

Forecasting techniques can be broadly categorized into (i) statistical or time series-based methods, (ii) physical methods, and (iii) hybrid or ensemble methods. However, machine learning (ML) techniques have by far outperformed the other categories. These include a large variety of artificial neural networks (ANN). They start from the well-known multilayer perceptron (MLP), the support vector machine (SVM) [6], the Markov chain methods, etc. ANN-based forecasting is generally considered very effective because of the ANNs' ability to learn complex, nonlinear relationships [2] and their significant advantage of being universal approximators [7]. The specific application requirements should be considered in the selection of the most suitable forecasting methodology. However, every successful forecasting model should be characterized by low computational expenditure and should be able to incorporate empirical knowledge. Further, it should be flexible and straightforward in the interpretation of its results [4]. The models proposed in the literature can be classified into two categories: trend methods and similar-day approaches [5]. Trend methods interpolate the demand curve as a function of time and extrapolate the curve to predict future demand. The similar day approach tracks similarities between current and historical load curves. Machine learning techniques fit this second category. A training set is formed in order to optimally determine or fit the model parameters. After sufficient training, the tuned model is applied to the test dataset. If the modeling error exceeds the set tolerance, the training set is modified, and the model is trained again. Aiming at the reduction of forecasting errors, many researchers proposed hybrid models. These models combine a clustering algorithm and a forecaster. The clustering algorithm captures characteristic attributes of the data. These include outliers, periodic behavior, and other relationships. The training set is divided into a number of relatively homogenous clusters. Each cluster set is employed to train its own forecaster. This process results in improved training of each forecaster. Time series models or ML models can be employed as forecasters in this process. The self-organizing map (SOM) can be profitably combined with SVM for peak load prediction. Fan et al. exploited an SOM for the categorization of their training data [8]. Separate support vector regression models are applied to each cluster to predict the daily peak load. Che et al. [9] combined the SOM and the support vector regression (SVR) with adaptive fuzzy rule forecasting and applied it to cases with variable training period lengths. The seasonality of load peaks is addressed through a functional clustering technique. Mori et al. [10] combined the deterministic annealing (DA) clustering for the preprocessing of input data, together with an MLP ANN, to predict day-ahead peak load. Kim et al. [11] classified existing seasonal load data into four patterns using Kohonen NN. Daubechies D2, D4, and D10 WTs were adopted subsequently to predict hourly load. Martinez—Alvarez et al. [12] applied clustering techniques to group and label the data set samples. Thus, the prediction of a data point starts with the extraction of the pattern sequence prior to the day to be predicted. Traditionally, most models were based on feed-forward (FF) ANNs trained by modification of the basic back-propagation algorithm. Cecati et al. [13] assessed five different learning algorithms for radial basis function (RBF) ANNs to advance their performance in the load forecasting of the ISO-New England market. Typical RBF networks were applied to 24 h electric load forecasting based on SVR, Extreme Learning Machines, and Decay RBF NN. In addition to the shallow and deep, fully connected FF ANNs, which are routinely employed in load forecasting, more complex types, such as the long short-term memory (LSTM), which is a version of recurrent neural networks (RNN), adopt a block structure with a number of gates interacting with the previous and next network state. They are more complex compared to FF ANN. However, they are capable of effectively handling temporal dependencies between variable time series lags. For this reason, they are employed in more complex forecasting tasks, such as the electricity price forecasting in auctions [14]. To this end, convolutional neural networks (CNNs) using convolution to learn patterns within specific time windows are also employed to learn from the data from different perspectives via data shuffling. A review of more recent developments with the use of deep learning (DL) methods in electric power systems is presented in [15]. Mishra et al. [16] analyzed the taxonomy of existing DL algorithms applied to different forecasting problems in the electrical utility industry. Khodayar et al. explored the theoretical advantages of deep learning in power systems research. Supervised, unsupervised, and semi-supervised applications, as well as reinforcement learning tasks, were covered [17]. Sun et al. [18] combined Bayesian probability theory and deep learning in a framework employing clustering in sub-profiles to forecast aggregated net load from the Ausgrid distribution network. Input data for the numerical experiments were collected from smart meters in load centers in Sydney, New South Wales. Additional input from residential rooftop PV outputs was considered to enhance the performance of aggregated net load forecasting. In spite of the significant research effort allocated to the structure of the ANN applied in the load forecasting problem, the structure of input data employed for the training dataset did not receive the necessary degree of attention. The majority of the research effort uses standardized input data from data repositories and performs benchmark tests to assess possible improvements in error metrics. On the other hand, the nature of the load forecasting problem on a country or regional basis is very complicated and affected by multiple factors discussed in the next section, in modes that are not yet well understood [19]. Moreover, day-ahead load forecasting on a country or regional level was challenged by the advent of COVID-19 and the associated shutdown of economic activity, which complicated the prediction. The period from March 2020 to May 2022 had peculiar characteristics due to the COVID-19 pandemic and the measures taken during large time intervals in order to protect public health from the spread of the virus. A study of the effects of shutting on and off several activities, aiming to assess the calibration capabilities of the prediction models, is still underway [20]. Surakhi et al. [21] investigated the dependence of forecasting accuracy on the selection of an optimal time-lag value. They comparatively tested a statistical approach using auto-correlation, LSTM, and a heuristic optimization algorithm combined with LSTM. In a comprehensive study involving data from load datasets from Australia, Germany, and America, Li et al. [22] tested a convolution-based DL model with a densely connected network. The model's backbone is the unshared CNN and a densely connected structure to avoid the vanishing of the gradient. Pavicevic et al. tested various models in temporal convolutional (TCN) and RNN/LSTM architectures for predicting the electricity price on the Hungarian market and electricity load in Montenegro TCN and LSTM layers, both in combination with fully connected layers, demonstrated the best performance, but in cases where all models failed with large mistakes, autoregressive LSTM performed even worse [19]. Mir et al. [23] presented the systematic development of a short-term load forecast (STLF) model using 5-year hourly load time series for an electric power utility in Pakistan. Following the investigation of previously developed models, they addressed the challenges of STLF by comparatively applying multiple linear regression, bootstrap aggregated decision trees, and ANNs.

Guo et al. [24] employed electricity consumption data from three cities in Jiangsu, China, to train a DL-based framework, random forest, and gradient boosting machine to forecast the total electricity consumption of 3000 users. To address various factors affecting residential electricity consumption, they used feature engineering. The influencing factors were divided into date-related and air-quality-related factors, weather factors, and local economic factors. As long as the forecasting is applied to large regions or a country level, the attainable accuracy is inferior. This is true, especially when the error metrics are applied to the hourly values of power demand. Wang et al. [25] applied a stacked noise suppression auto-encoder (SDA) model and a class of DNN to forecast the hourly electricity price. The datasets were compiled from hubs in five U.S. states. Two types of forecasting, online hourly forecasting and day-ahead hourly forecasting, were examined. MAPE values in the range from 2.51% to 46% were reported, depending on the price fluctuation, which was very high in January and very low in April 2014. Hossen et al. [26] employed a DNN for forecasting day-ahead electricity consumption. Ninety days of data from the Iberian utility market were employed for training the multilayer DNN.

Various combinations of activation functions were tested, aiming at improved MAPE, taking into account the weekday and weekend variations. The functions tested include Sigmoid, rectifier linear unit (ReLU), and exponential linear unit (ELU). Weekday MAPE ranged between 2.1 and 3.9%. Weekend MAPE ranged between 1.3 and 2.5%. Din and Marneridis [27] investigated the feasibility of the application of the feed-forward DNN and recurrent-DNN models utilizing datasets from ISO New England. The proposed models obtained the least daily demand prediction MAPE errors of the order of 1% in the spring season. The highest errors were observed in the summer. They were attributed to the unexpected electricity consumption exceedance caused by high temperatures and social events. Dong et al. [28] combined CNN and K-means algorithms to predict hourly load. They applied the K-means algorithm to a 1.4 million electrical load records dataset, restructuring it into several subsets. Afterward, these subsets were input to CNN for training and testing. The results were promising, attaining 3% MAPE during summer and 7.4% MAPE during winter. Wen et al. [29] employed deep RNN–gated recurrent unit (GRU) models for short- and medium-term prediction, which attained a MAPE of 3.5% in their forecasts. Kong et al. [30] made short-term load predictions at the individual building level. They applied a density-based clustering method to calculate and compare the inconsistency between the combined load and individual loads. Since the consumers' lifestyle significantly changes the energy consumption pattern, the authors proposed an LSTM–RNN-based load forecasting structure for the load demand dataset. The LSTM and BPNN-T in the top tier outperformed all the other benchmarks: MAPE varied from 8.18% to 8.64% in the predictions. Shi et al. [31] proposed a pooling-based deep-RNN for household load forecasting. They attempted to avoid over-fitting caused by increasing data diversity and dimensions. Their STLF model was tested on 920 residential smart meter datasets in Ireland. The RMSE attained outperformed ARIMA by 19.5%, SVR by 13.1%, and classical deep RNN by 6.5% in terms of RMSE. Peng et al. [32] presented a useful comparison of important research works on typical methods used in electricity load forecasting, with indicative values of statistical metrics. They developed and applied a hybrid method—improved backtracking search optimization algorithm (IBSA)–double-reservoir echo state network (DRESN) in STLF. Mutual information is utilized to eliminate low-significance input features and retain key input features. The DRESN structure aims to increase the diversity of the network. Roulette strategy, adaptive mutation operator, and niche operator are introduced to improve the standard BSA algorithm. The IBSA is applied to optimize several critical parameters in the DRESN neural network. The proposed method outperformed eight popular benchmark models, as tested with North America and PJM load datasets. The decades of development of short-term electricity load forecasting techniques have been invested in flexible and easy-to-use computational tools currently employed by the network operators [33]. However, as reported above, the prediction accuracy needs further improvement regarding the design and implementation of the input training datasets, which have specific peculiarities for each country, depending on the size, climate, and economic activities' diversity and other factors. As seen in the above presentation, modeling error results reported from several research works in short-term electrical load forecasting vary over a wide range of MAPE and nRMSE. This can be attributed to the wide variation of training input data structures and the different types of predictions obtained and the different geographical scales met in the different applications. The focus of the present work is on further improvement and standardization of the training dataset of the day-ahead load prediction. This is accomplished by adding the daily heating and cooling degree-days of a representative location, as well as improving the prediction of the peak load, after carefully studying specific time periods in the Greek system where all models systematically fail. In this process, two standard, popular, and cost-effective FF ANN models are employed for the day-ahead system's load forecasting. The comparison is carried out using consistent metrics and the same data from the Greek system [34]. The hourly actual aggregate electricity load, as reported by the Greek Independent Power Transmission Operator (IPTO) [34] during the five-year period 2017–2021, was employed in the training of the models, along with meteorological data. Testing and validation of the models are carried out for various periods of 2022. The main contributions of the present work are the following: (i) the current prediction accuracy level attained in the Greek system is not high, and it is proven that it can be easily attained with simple types of FF ANNs and easily available datasets; (ii) a systematic procedure is adopted to find and discuss the most important incidents of prediction failure, explain the reasons of failure, and indicate possible pathways to their remedy. (iii) This procedure leads to suggestions for improvement in the selection and phasing of the training variables, the increase in data monitoring frequency, and the possible inclusion of information on specific economic activity variables to be included in the training and prediction. The paper is organized into four sections. Section 2 presents the overview of input data and the formulation of the prediction methodology to be employed. Section 3 discusses the selection of input data and the specific types of ANN for the day-ahead forecast. The results of the simulation are presented and discussed in Section 4. Finally, the conclusions and future work are presented in Section 5.

2. Materials and Methods

Before attempting to formulate a day-ahead load prediction methodology, it is useful to present and discuss the current state of the day-ahead prediction of Greece's electricity load curve, as reported to the European Transparency Platform (ENTSO-E), which is responsible for the central collection and publication of Electricity Generation, Transportation, and Consumption Data and Information for the Pan-European Market [35]. As an example, the actual demand values, on an hourly basis, are compared with the day-ahead predictions for January 2022 in Figure 1. The average values and variability, on a monthly basis, of the most important statistical metrics for 2022 are shown in the same Figure to quantify the prediction accuracy. MAPE is 2.61% with a standard deviation of 0.33%, and nRMSE is 0.036 with a standard deviation of 0.005. Finally, the mean bias error (MBE) is 73 MW, which indicates an over-prediction. On a qualitative basis, it is interesting to see in this example of January 2022 (Figure 1) that the most pronounced prediction failures are observed with regard to the morning peaks, and to a much lesser extent, to the late afternoon peak loads. It must be mentioned in this respect that the specific level of prediction accuracy is not attained by a truly day-ahead computation. That is, not all 24 h of the next day are predicted. Instead, the next day's prediction is corrected at noon, based on the—known at that time—actual load data of the first half of the day.

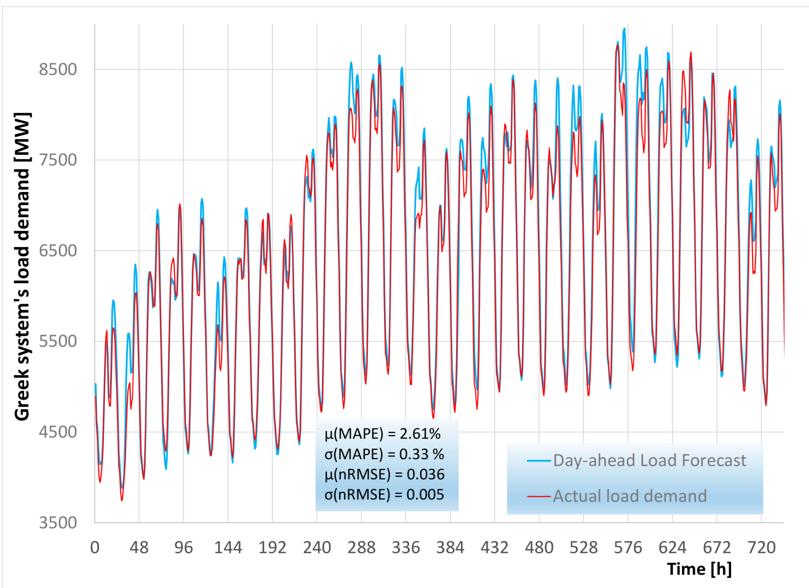

Figure 1. Greek system load during January 2022, day-ahead predicted versus actual values (MW) [35].

The effect of this improved prediction may be seen in the example of a typical weekday (20 January 2023) based on the data reported daily by the Greek system operator (IPTO) [34] presented in Figure 2. The modified noon prediction reduces the 24 h MAPE from 3.35% to 2.47% and nRMSE from 0.041 to 0.035. Thus, the forecasts reported in the ENTSO-E database are not true 24-hour-ahead forecasts. This explains the somewhat reduced accuracy in our true 24-hour-ahead forecasts presented in the next section.

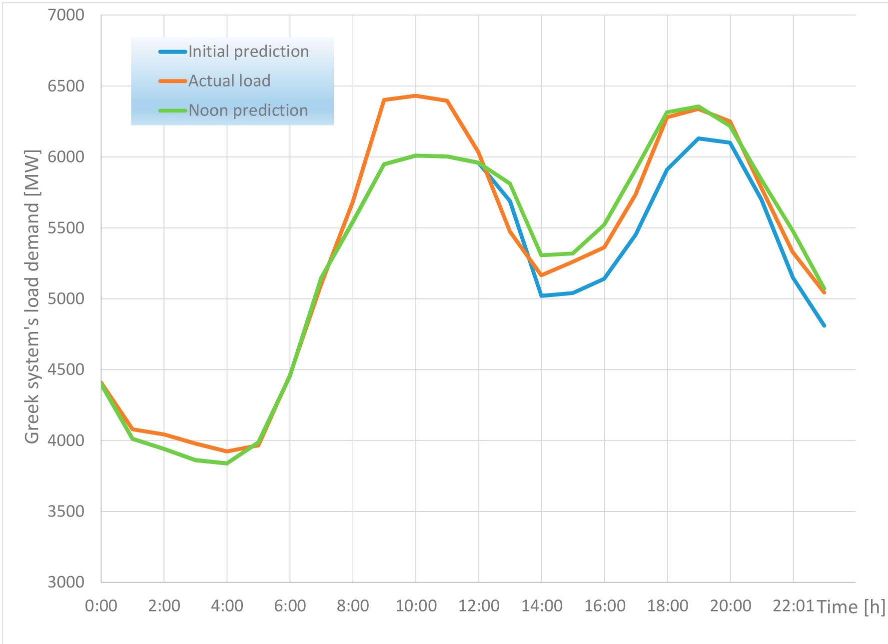

Figure 2. Initial day-ahead prediction, modified noon prediction, and actual load curve on a weekday in January 2023 [34]. The modified noon prediction reduces 24 h MAE from 177 to 131 MW, MAPE from 3.35% to 2.47%, and RMSE from 0.041 to 0.035.

Before proceeding to study the accuracy of the prediction of special events and spot-specific cases of prediction failure, it is important to understand the general typologies of the Greek system load curves in the main seasons of the year.

2.1. Typical Load Curves of the Greek System, Seasonal Effects

To understand the behavior of the 24 h total electric load curve, its evolution during a Friday of January is shown in Figure 2. The total system's load drops during the night, stabilizing at about 3.9 GW. The minimum values are before dawn, from 3:00 to 5:00 in the morning. This base load level makes up for the night consumption, which covers the following main activity:

- Urban, road, and highway lighting;
- Industrial production continuing to the night shift;
- Base load of the residential sector.
- Refrigeration loads for the industrial, commercial, and residential sectors.

In the period 05:00–09:00, we observe the morning ramp. During the noon hours, the demand drops below 5.4 GW. From 16:00 to 18:00, the afternoon ramp leads to a demand plateau close to 6.3 GW between 18:00 and 20:00. Next, it is useful to study the patterns of another day, which is a Monday in November (Figure 3).

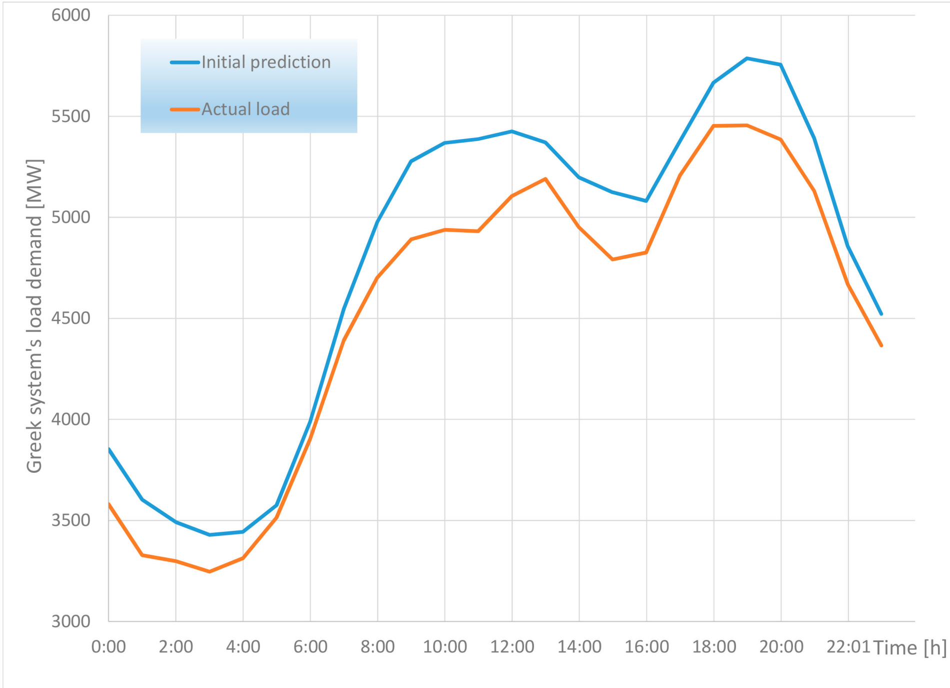

Figure 3. Evolution of the Greek system load on a typical Monday of November, 2022. Predicted versus actual hourly load values [35].

The behavior of the demand curve during the night is about the same. However, the base load during the night drops below 3.5 GW. The morning ramp during this weekday is characteristic, with a total demand increase of 1.25 GW between 05:00 and 08:00. The morning ramp continues more gradually to the first load peak of the day (about 10:00 AM). This corresponds to the following activity:

- Industrial activity starts for the morning shift.
- Commercial and services activity starts.
- People prepare and go to work.
- Students prepare and go to school.
- Space heating starts after the night shut down.

After 9:00 AM, we observe an approximate consumption plateau, which results in a daily minimum at about 3:00 PM. Following the noon hours, we observe a gradual increase in consumption, which leads to the second ramp of the day and leads to the second consumption peak at 18:00–19:00 (because of the winter time and the early advent of evening, while this peak goes up to 21:00–22:00 during summer time). This second peak reaches 5.5 GW during this mild late autumn day but may reach 8.5 GW or more during winter (Figure 1) due to the part of space heating supplied by electricity. After 8 PM, we observe a gradual reduction in the electric load, which takes its night levels after 02:00.

The system's load levels may drop significantly lower during the neutral months of April–May and October, respectively, which do not require electricity consumption for space heating in the residential and part of the commercial sector.

An example of this performance is presented in Figure 4 for the month of April, 2022, where the minimum demand during the night drops close to 3 GW and the evening peak drops to less than 6 GW during late April, where ambient temperatures are of the order of 20–24 °C during the day.

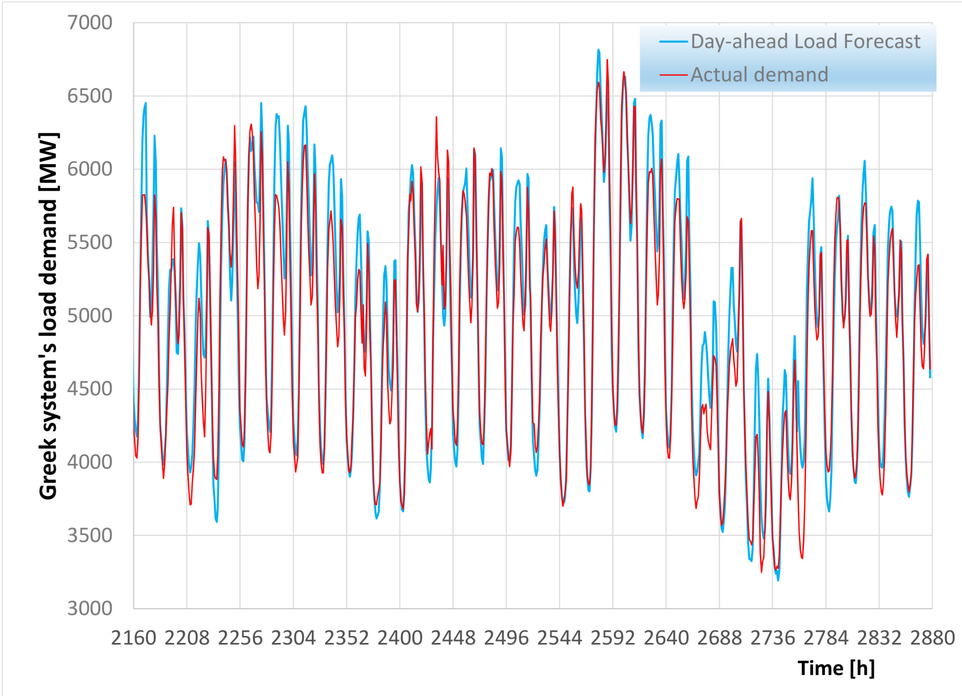

Figure 4. Greek system load during April 2022, day-ahead predicted versus actual values (MW) [35].

Further, it is interesting to observe in Figure 5 a pronounced load prediction failure of the Greek system's operator for the period 20–22 April (Wednesday to Friday, hours 2640–2712). An observation of the weather data for typical places in central Greece shows a sudden weather improvement after a rainy and cold weekend. A closer observation of this period in Figure 5 indicates that the day-ahead prediction routinely over-predicts the demand for the 20th, 21st, and half of the 22nd of April.

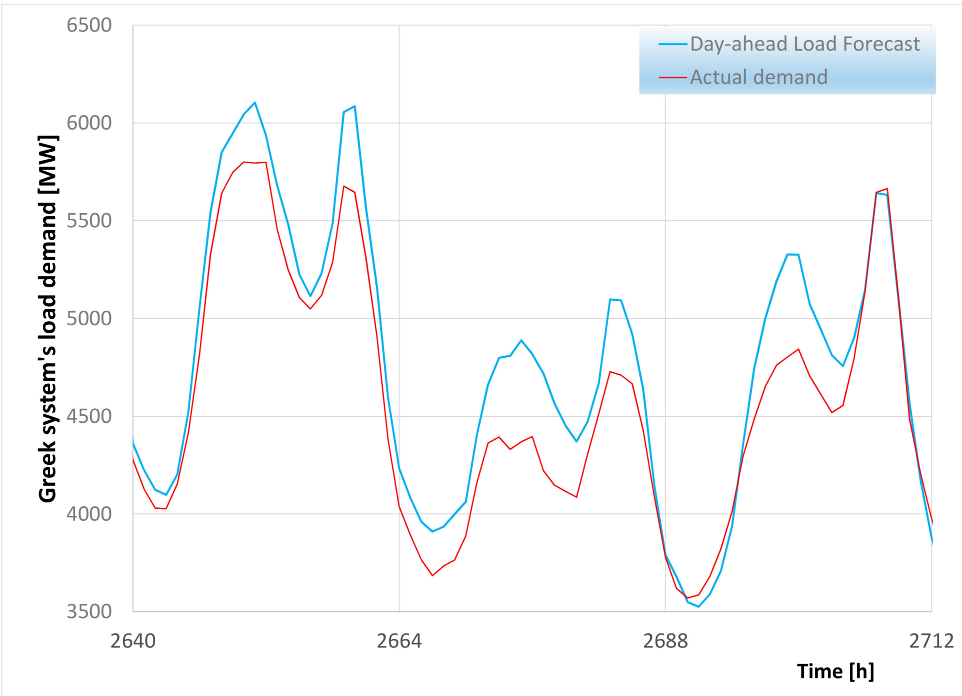

Figure 5. Load prediction failure during the period Wednesday 20 to Friday 22 April, 2022 (sudden weather improvement) [35]. Maximum relative error is 11.9%.

Only after the noon correction in the prediction of the afternoon system's demand the error vanishes, and the prediction accuracy returns to high levels.

Next, the Greek system's operator's forecasting is compared with the actual demand for the month of July 2022 (Figure 6). This is a difficult period for forecasting because of the high electricity demand for air conditioning, which leads the system's peak demand to exceed 9 GW for certain cases (25–28 July, hours 4920–5016). As regards the prediction accuracy, it is interesting to observe a prediction failure for the weekend 16–17 July (hours 4704–4752), which is shown in detail in Figure 7.

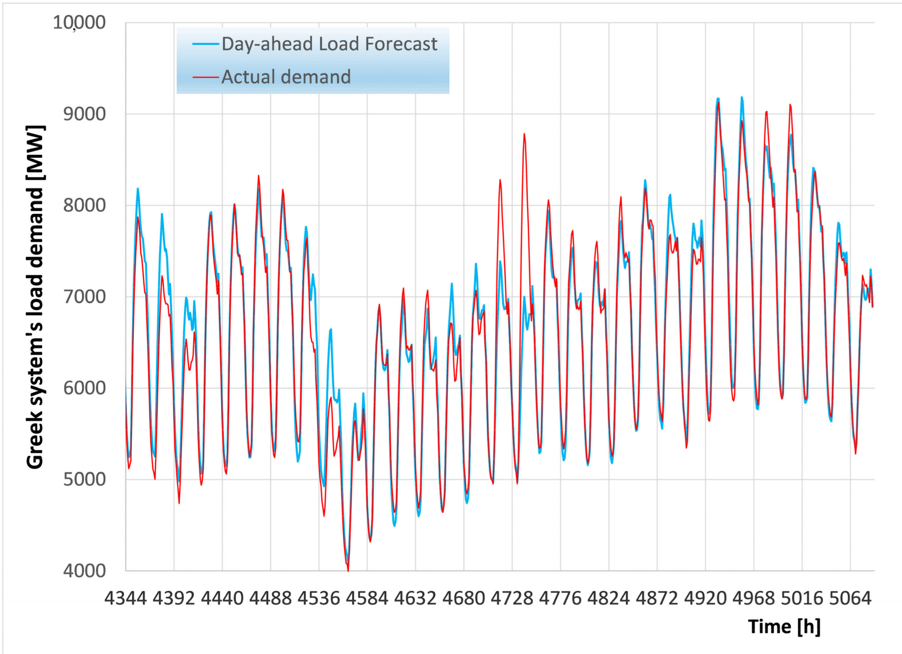

Figure 6. Greek system load during July 2022, day-ahead predicted versus actual values (MW) [35].

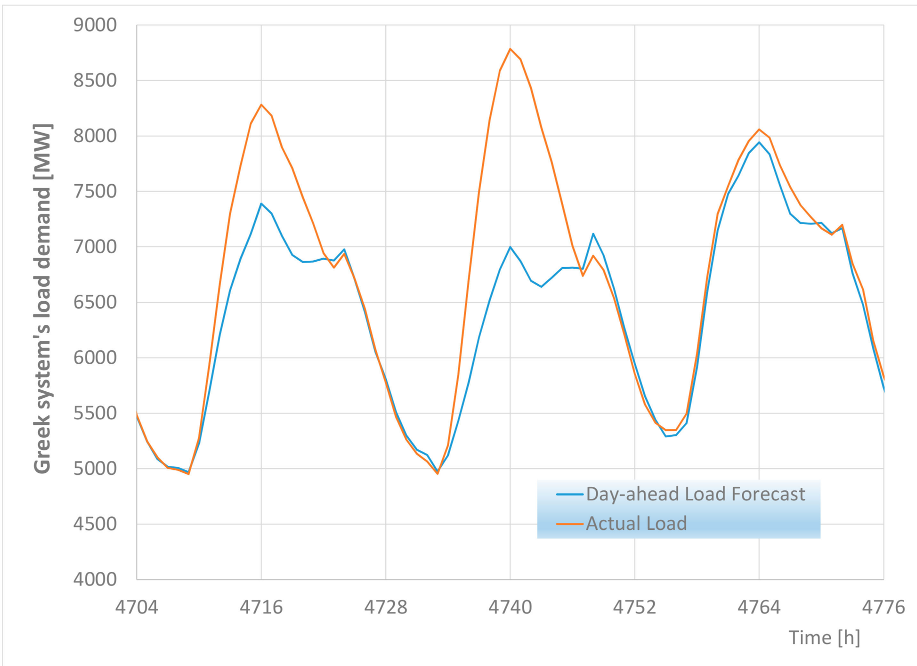

Figure 7. Prediction failure for the period during the weekend 16–17 July with high ambient temperatures [35]. Maximum relative error is −20.9%.

The system's operator failed to predict with sufficient accuracy the effect on the system's demand of the onset of high ambient temperatures during the specific weekend. This will be examined in more detail in view of the respective predictions of our models in Section 4. Next, we are going to present the modeling approach we developed and tested, aiming at further improving the forecasting accuracy of the Greek system demand.

2.2. Input Data Employed for the 24-Hour-Ahead Forecasting

Our investigations were based on the processing of the measured hourly electrical load during the years from 2017 to 2021, for which the hourly load demand input data for the Greek system were obtained from ENTSO-E [35]. Testing and validation of the models were carried out for various months in 2022. In addition to the electric load curves, meteorological data, at least on a daily basis, need to be employed for representative climatic conditions of Greece. The central location of Athens in Greek geography, and the presence of about 40% of the population and a significant part of industrial and business activity here, allows us to consider Athens weather data as corresponding—more or less—to the average Greek climate as weighted by the number of inhabited space and number of inhabitants. For this purpose, out of the four weather stations of the central Athens area (Gazi, Ambelokipi, Patissia, Psychico) [36], the suburb of Psychico was selected for weather data [37]. Psychico may be considered as representing the climatic conditions of Athens, which hosts a major part of the population and economic activity, and, on the other hand, its climate is not severely affected by the city-center conditions. On the other hand, because it may be considered to belong to the northern suburbs, and it is not densely built with high-rise buildings, and it has plenty of trees and park space, its climate is not affected by Athens center conditions, a fact that allows it to be more representative of Greece. For this reason, input weather data as daily averages and high-low temperature values were obtained from the meteorological station of Psychico [37].

Apart from meteorological variables such as dry bulb temperature and relative humidity, load presents a high correlation to its past values [4]. To this end, it is interesting to confirm, to the specific dataset, the generally observed short-term periodicity of the load using the Pearson correlation coefficient [38]. In Figure 8, the Pearson correlation coefficients of the current hourly load for the full year 2021, correlated with its previous hourly values up to 216 h before, are graphically presented. Obviously, they start from the value of 1 at zero delay, and they are seen to fluctuate with 24 h periodicity. However, a high correlation coefficient of 0.9344 is clearly observable for a 24 h delay. Next, a higher correlation coefficient observed was 0.8392 for a 168 h delay. For this reason, 24 h lagged load and 168 h (previous week) lagged load are routinely fed as input to FF ANN applied for day-ahead load prediction.

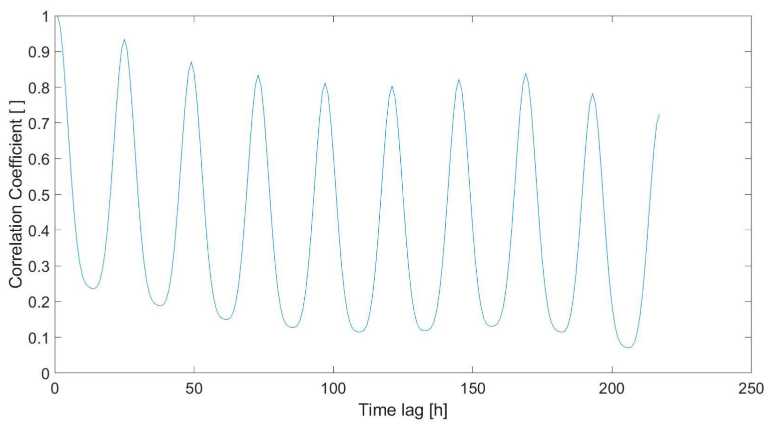

Figure 8. Correlation coefficient curve for evaluating short-term periodicity characteristics of the Greek system load curve for the full year 2021. Strong correlation exists with the 24 h lagged load (previous day) and, to a lower extent, with the 168 h lagged load (previous week).

For the day-ahead load forecast, the following are input parameters usually applied in the specialized literature:

- Dry bulb temperature;
- Dew point temperature;
- Hour of day;
- Day of the week;
- Holiday/weekend indicator (0 or 1);
- Previous 24 h average load;
- 24 h (previous day) lagged load;
- 168 h (previous week) lagged load.

The ambient dry-bub (DB) temperature is included in most investigations because temperature affects electricity consumption. The correlation between the total daily electricity demand (GWh) of the Greek system in 2021 and daily average temperature is shown in Figure 9. A nonlinear relationship between load and temperature is observed. There exists a baseline daily demand of the order of 100–130 GWh, during the days with normal average temperature (DB) in the range 18–24 °C. With the onset of higher average temperatures, the total daily load steeply increases up to 210 GWh.

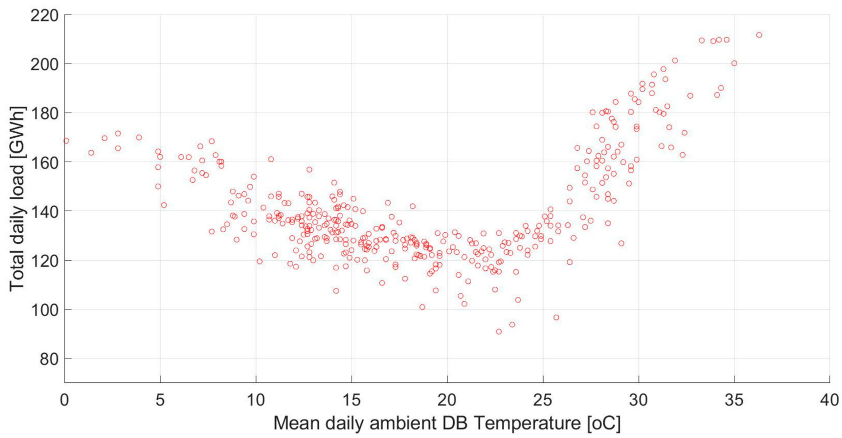

Figure 9. Correlation of the total daily electricity load in GWh with the daily mean temperature (DB) of Psychico weather station (year 2021).

The same trend is observed when the mean daily temperature deviates to values lower than normal. However, as seen in Figure 9, the effect of lower mean daily temperature levels on the total daily load (GWh) is significantly less pronounced. This is due to the fact that space cooling is carried out almost exclusively by means of electrically driven heat pumps and air-conditioning equipment, whereas the heating is mainly carried out by natural gas, oil and pellet-fueled boilers, and—to a lesser extent—by heat pumps or split units in heating mode. Hourly temperature data (dry bulb and dew point) for locations in high-demand areas of the system are usually considered. Another environmental variable that affects electricity consumption is the ambient air humidity, usually reported in the form of more complex indices such as the relative humidity (RH), dew point (DP) temperature, or wet bulb (WB) temperature. However, the correlation of any one of these indices with the total load is not straightforward. On the other hand, since the effect of ambient temperature and humidity on the electricity consumption is conveyed through the heating or cooling requirements, we considered, as a good practice, to correlate the total daily load in GWh with the heating degree-days instead. These are routinely reported on a daily basis by all weather stations. This correlation is presented in Figure 10 for a typical weather station in the Athens area during 2021.

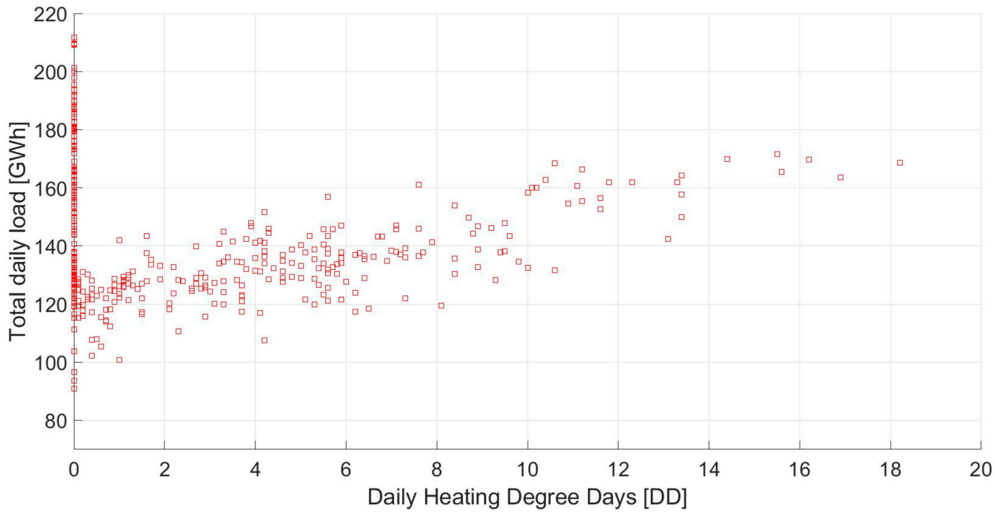

Figure 10. Correlation of the total daily electricity load in GWh with the daily heating degree-days (Psychico station, year 2021).

As seen in Figure 10, the correlation of the total daily load with the daily heating degree days during the heating season is significantly better than the correlation with ambient temperature seen in the previous Figure. This hints at a possibly better training ability of the machine learning models to be employed in the predictions.

Moreover, cooling degree days are also reported on a daily basis by all weather stations since they give an estimate of the necessary energy consumption for space cooling during the summer. Again, a correlation of the total daily load in GWh with the cooling degree days of a typical weather station in Athens, shown in Figure 11 reveals a clear positive correlation whenever five cooling degree days are exceeded daily.

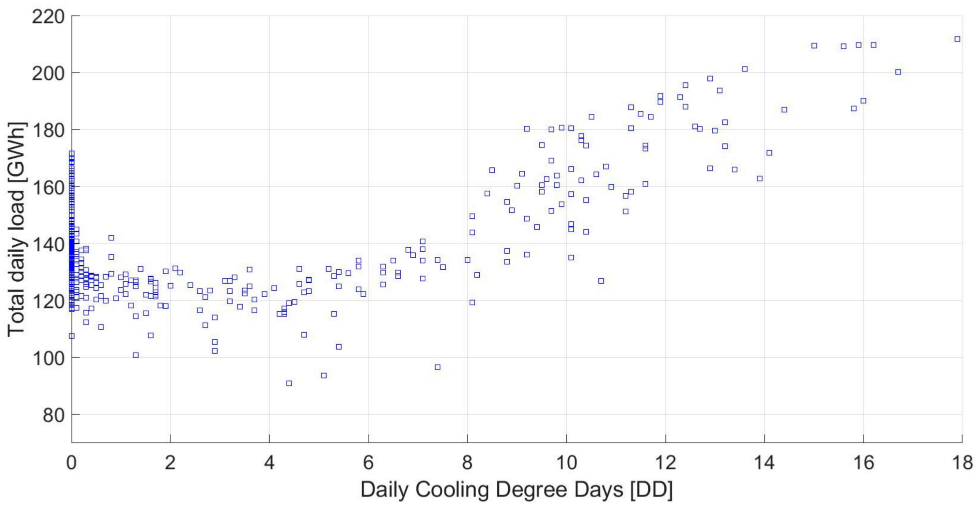

Figure 11. Correlation of the total daily electricity load in GWh with the daily cooling degree days (year 2021).

As already observed for the cooling season, the correlation coefficient of the total daily load with the daily cooling degree days is significantly higher than the correlation with the heating degree days. Based on the above findings, in the current work, we preferred to use the daily heating and daily cooling degree days instead of the DB and the DP temperature. The required weather data are significantly more simple and easy to acquire since they refer to just two daily values instead of the two 24 h vectors required by the usual practice. Moreover, the daily weather forecast required for the day-ahead forecast requires just a single value (daily heating or cooling degree days) instead of 48 values, involving the forecasted hourly values of DB and DP temperatures. To summarize our model training approach, the following input parameters are selected for training:

- Heating degree days (daily for a representative meteorological station);
- Cooling degree days (daily for a representative meteorological station);
- Hour of day;
- Day of the week;
- Holiday/weekend indicator (0 or 1);
- 24 h lagged load (hourly resolution);
- 168 h (previous week) lagged load (hourly resolution).

3. Neural Network Selection

As already discussed in the introduction section, a significant volume of research work has been carried out in the last decade, especially concerning the application of deep learning in the electrical utility industry, including power system fault detection and classification, load and power forecasting, wind speed and irradiance forecasting for wind and PV energy system, power quality detection, etc. As regards applications in short-term power load forecasting, the more advanced deep learning models are usually applied in specific cities or communities. On the other hand, the complex nature of the problem of electrical load forecasting on a country basis requires special attention to the type of data to be employed for the training. Since there is no possibility of reconstructing the problem of forecasting the total load demand of a country, with 1 h resolution, by adding a very large number of distribution units covering cities and counties that could be addressed with advanced ML models trained by numerous input data of more local character. Based on the above reasoning, our selected approach must be checked for effectiveness, starting from the simplest types of shallow neural networks and comparing them to the prediction accuracy of the state-of-the-art commercial forecasting platforms.

To this end, the following two types of simple, feed-forward ANNs were selected for comparative testing in our investigations.

3.1. FF ANN

Due to the fact that the above-mentioned inputs must be assimilated in a complex way to match the training target points, a feed-forward neural network is very well suited for this type of time series forecasting. Neural networks have a proven ability to fit multi-dimensional mapping problems arbitrarily well, given consistent data and enough neurons in their hidden layers. The first neural network to be applied is the well-known, simple form of a feed-forward artificial neural network (FF ANN) with one hidden layer, or MLP, with sigmoid hidden neurons and linear output neurons.

The values of several important parameters of the FF ANN employed are presented in Table 1. The network training function updates weight and bias states (expressed in vector form x_k) according to the Levenberg–Marquardt back propagation optimization algorithm [39]:

$$x_{k+1} = x_k - \left[J^T(x_k)J(x_k) + \mu_k I\right]^{-1} J^T(x_k)v(x_k) \tag{1}$$

where J is the Jacobian, μ_k is the value of mu at step k, and $v(x_k)$ is the vector of the components of the modeling error (sum of squares) [40]. As μ_k is increased, the algorithm approaches the behavior of the steepest descent algorithm with small learning rate [39]:

$$x_{k+1} \cong x_k - \frac{1}{\mu_k} J^T(x_k)v(x_k) = x_k - \frac{1}{2\mu_k}\nabla F(x) \tag{2}$$

as μ_k decreases to zero, the algorithm becomes Gauss–Newton.

Table 1. Design parameters of the specific type of FF ANN applied, along with the hyper-parameter values related to the training procedure.

ANN Type	FF
ANN Dimensions	
Inputs	7
Layers	2
Outputs	1
Input Delays	0
Layer Delays	0
Weight Elements	160
ANN connections:	
Bias Connections:	[1; 1]
Input Connections:	[1; 0]
Layers Connections:	[0 0; 1 0]
Output Connections:	[0 1]
ANN Training hyper-parameters	
Maximum Epochs	1000
Maximum Training Time	Inf
Performance Goal	0
Minimum Gradient	1.00×10^{-7}
Maximum Validation Checks	6
μ_k	0.001
μ_k decrease ratio	0.1
μ_k increase ratio	10
Maximum μ_k	1.00×10^{10}

The algorithm begins with $\mu_k = 0.001$ (Table 1). If a step does not yield a smaller value for the modeling error, the step is repeated with μ_k multiplied by a factor of 10 (Table 1). If a step reduces the modeling error, then μ_k is divided by 10 for the next step. Thus, we approach Gauss-Newton, to provide faster convergence. The algorithm provides a nice compromise between the speed of Newton's method and the guaranteed convergence of the steepest descent.

The FF ANN is implemented by the use of the open-source platform Tensorflow [41]. The input layer includes seven input nodes, namely, heating degree days, cooling degree days, hour of day, day of week, holiday/weekend indicator, 24 h lagged load, and 168 h lagged load. The hidden layer comprises 20 neurons, each containing a sigmoid activation function [42]. Training involves the fitting of a complex curve through the training data. This is affected by employing loss minimization algorithms, as well as the corresponding weights and biases optimization. Since this type of complex fitting procedure is employed in the day-ahead prediction, it excludes erroneous or noisy information from the dataset. This explains why the required quality assurance procedure must be included in the preprocessing of the reported electricity demand data to correct any reporting errors or missing values [43–45]. Validation is performed with one dataset, which corresponds to the actual demand year 2022. In the specific runs, we did not consider overfitting, which would require further validation datasets and observation of possible decrease in the modeling error associated with an increase in the validation error [46].

3.2. Feed-Forward Back Propagation Neural Network

A more complex type of neural network examined is a feed-forward back-propagation neural network (BPNN) with two fully connected hidden layers [47]. This type of network has already been successfully applied to forecasting problems of complex systems with highly nonlinear behavior affected by several parameters [14,48,49]. For a single-layer network, the error is an explicit function of the network weights, and its derivatives with respect to the weights can be easily computed. In multilayer networks with nonlinear transfer functions, the relationship between the network weights and the error is more complex [39]. The goal of BPNN is to update each of the network weights so that the neural network can approximate its output to the desired target. The error between the neural network output and the desired target can be written in the form of a cost (or loss) function, where O_k is the output and t_k is the desired target for a specific time step:

$$E = \frac{1}{2} \sum_{k \in K} (O_k - t_k)^2 \tag{3}$$

The objective is to minimize this cost function by updating the weights and biases during the training process, which, for the specific type of network, is an iterative process. It starts with forward propagation with the training dataset, which computes an initial output and then compares it to the reference values (targets) to calculate the loss function. The loss is back-propagated using a series of partial derivatives with respect to each FNN's internal parameters (weights and biases). Thus, the values of these parameters are updated, and a new iteration starts. The iterative process ends with the fulfillment of convergence criteria or when the maximum number of epochs is attained. At regular intervals during the training iterations, a separate test dataset is employed to validate the accuracy of the BPNN. This procedure is similar to the one employed to train the feed-forward ANN described in Section 3.1.

The Adam optimization algorithm is employed for training the specific ANN, as mentioned in Table 2. It is an extension of the classical stochastic gradient descent procedure, which computes individual adaptive learning rates for different parameters from estimates of the first and second moments of the gradient [50]. Training methods with a derivative-based optimization algorithm, such as Levenberg–Marquardt or Adam, may be trapped in local minima; hence, they should be repeated to ensure they lead to an appropriate ANN.

Table 2. Design parameters of the deep BPNN, along with the hyper-parameter values related to the training procedure.

ANN Type	**FF BPNN**
ANN Dimensions	
Inputs	7
Layers	5
Hidden layers	2
Outputs	1
Number of hidden neurons	55
ANN connections:	
Layer Connections:	Fully connected
Normalization layer	z-score
Additional Layer	tanh layer
Additional Layer	leaky ReLu layer
ANN Training hyper-parameters	
Maximum Epochs	1000
Maximum Training Time	Inf
Performance Goal	0
Learning Rate Drop Period	400
Initial Learning Rate	0.01
Learning Rate Drop Factor	0.1
Mini-batch size	1
Solver type	Adam
Validation frequency	30

A comparative analysis of the results of applying the two types of networks with the actual demand for various periods of 2022 takes place in the next section and is based on the MAPE and the nRMSE error metrics. This type of performance metric is routinely applied in load forecasting problems. They are expressed as follows:

$$MAPE = \frac{100\%}{N} \sum_{i=1}^{N} \frac{|Pf_i - Pm_i|}{Pm_i} \tag{4}$$

$$\mathrm{nRMSE} = \frac{\sqrt{\sum_{i=1}^{N}(\mathrm{Pf_i} - \mathrm{Pm_i})^2}}{\sqrt{\sum_{i=1}^{N}(\mathrm{Pm_i})^2}} \quad (5)$$

where $\mathrm{Pm_i}$ and $\mathrm{Pf_i}$ are the actual and forecasted loads of hour i, and i = 1,2 ... N is the sequential number of hours in the time period examined.

4. Results and Discussion

Indicative results of the two models are presented, along with the respective values of the modeling error metrics for 2002. All metrics are computed on the test datasets. In addition to these metrics, plots of the error distribution as a function of the hour of the day and day of the week are generated to spot specific weak points in the forecasting. The various plots comparing the day-ahead hourly actual and forecasted load for typical months for the year 2022 are generated and optically checked for specific instances of prediction failure.

4.1. FF ANN

As an example, the actual demand values, on an hourly basis, are compared with the day-ahead predictions with the FF ANN for January 2022 in Figure 12. The computation time was less than 30 s and the code converged after less than 100 epochs. The values of the respective statistical metrics for 2022 are shown in the same Figure to quantify the prediction accuracy. The RMSE was 3.08 MW, MAPE was 3.66%, nRMSE was 0.049, and MAE was 204 MW. Finally, MBE was 29 MW, which indicates a small over-prediction. On a qualitative basis, it is interesting to see that the quality of prediction for January 2022 was comparable to the prediction of the Greek system's operator, presented in Figure 1. Again, the most pronounced prediction failures are observed with regard to the morning peaks. It should be mentioned here that the specific, comparable levels of prediction accuracy were attained by a true day-ahead computation. That is, all 24 h of the next day were predicted. No correction at noon was applied in this case.

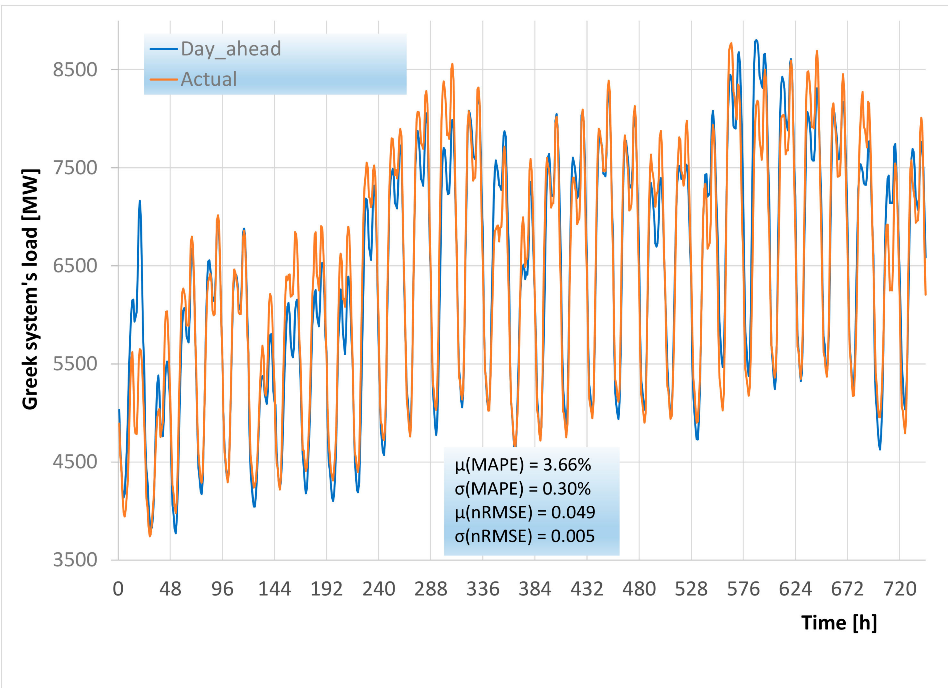

Figure 12. Prediction with the FF ANN and validation of the Greek system's demand for January 2022. MAPE and nRMSE means and standard deviations refer to the full year 2022.

Further, it is interesting to look at the variance of the most important error metrics in these predictions. To this end, Figure 13 presents the variation of the monthly MAPE and nRMSE values for the official forecasts in comparison with the respective figures for the FF ANN predictions. Although the mean values of MAPE and nRMSE were lower for the official predictions, the standard deviations were observably higher than the respective error figures of the FF ANN predictions. The reduced standard deviations in the FF ANN prediction error metrics are a good indication for the lack of data overfitting problems.

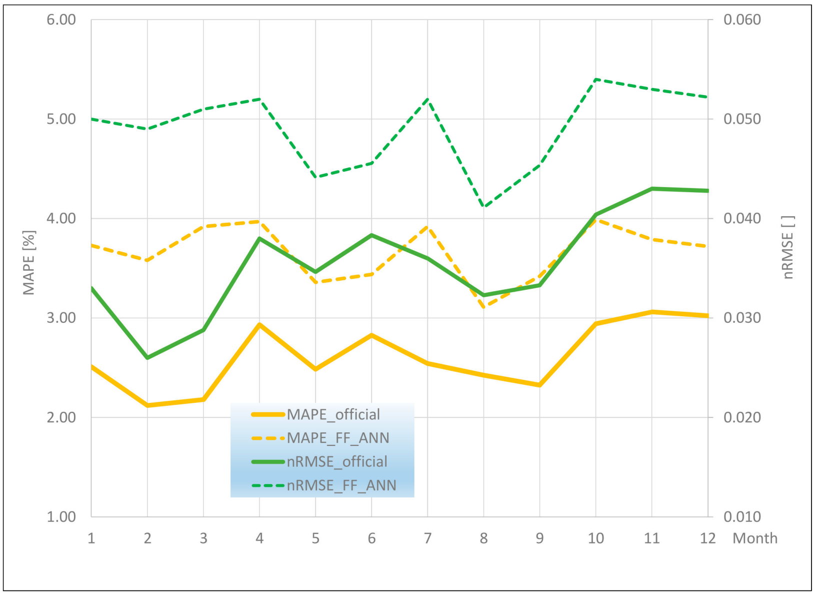

Figure 13. Comparison of the variation of monthly MAPE and nRMSE for the official forecasts and the FF ANN forecast during 2022.

Apart from the visual, qualitative inspection of prediction quality, it is interesting to statistically assess the effects of the hour of the day and the day of the week in the FF ANN prediction errors. In this context, Figure 13 presents a box plot of the error distribution of forecasted load as a function of the hour of the day for 2022. A closer look at the box plots of this figure confirms the intuitive observation that the prediction of the nighttime base load is most confident. The other important finding is that the maximum prediction error, reaching values of the order of 15%, was observed for the hours 16:00–18:00, which correspond to the interval of returning from work. Again, this is expected by visual observation and affects the prediction accuracy of the late afternoon peak of the Greek system, which is the most difficult to address. This suggests that a significant part of the research effort should be directed to the improved prediction of the peak load for the daily load curve.

As a second step in this direction, Figure 14 presents a box plot of the error distribution of forecasted load as a function of the day of the week for 2022.

A comparison of the respective error box-plots in Figure 15 reveals that the weekdays where the maximum prediction error is observed are Saturday (#7) and Monday (#2). The reduced accuracy in the prediction of Saturday may be attributed to the fact that Saturday and Sunday are both categorized as weekend days. However, although the behavior of the system's load on Sundays is very particular, lying in between the behavior of weekdays and Sundays. Thus, it would be helpful to find a way to inform the artificial neural network during the training about these differences. Simply allocating a third category for Saturday was tested but did not improve the model's prediction capabilities.

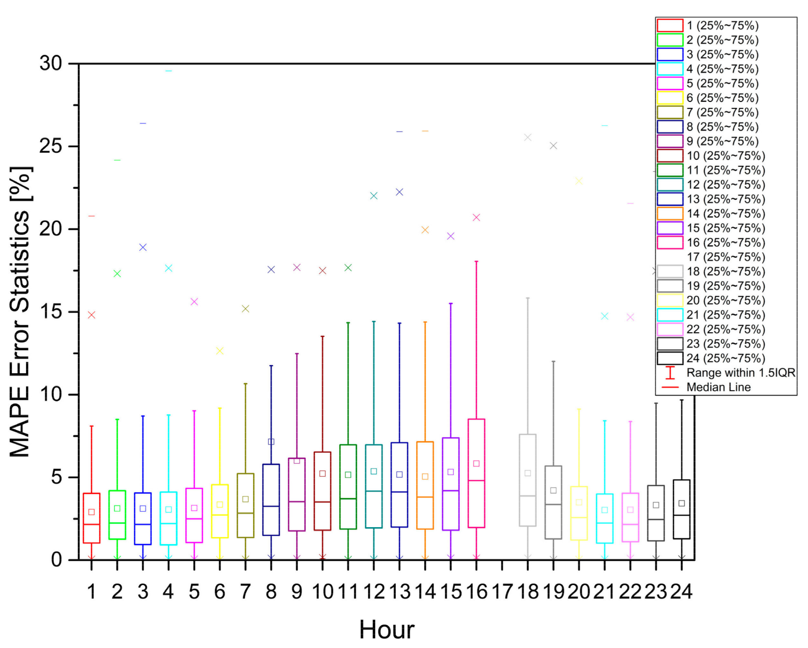

Figure 14. FF-ANN forecasting: Box-plot of the error distribution of forecasted load as function of the hour of day for 2022.

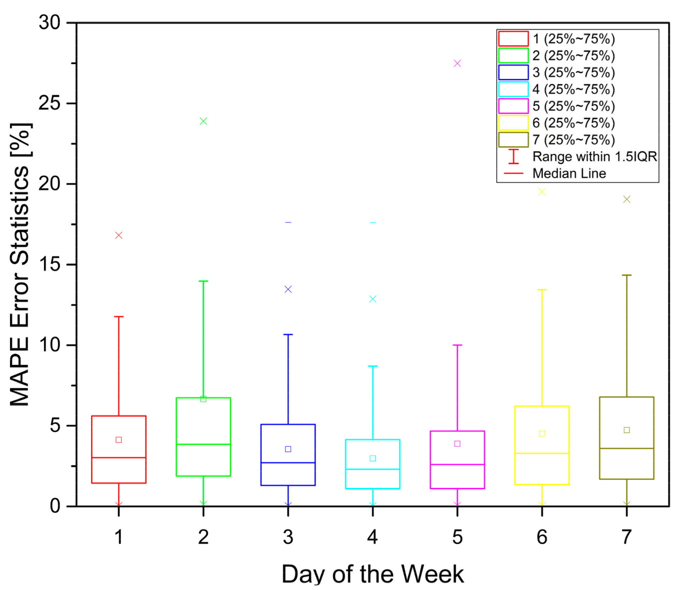

Figure 15. FF-ANN forecasting: Box-plot of the error distribution of forecasted load as function of the day of week for the year 2022.

4.2. Deep FF BPNN

The training progress of the two-hidden layers' FF-BPNN was tested by setting a different number of maximum epochs in the range 20–2000. The computation time was about an order of magnitude higher than the simple FF ANN; that is, it takes about 2 min to run 1000 epochs on a standard laptop PC. The results are presented in Figure 16 in terms of the attained RMSE of the normalized predicted values of load demand, which is seen to stabilize at a little higher than 0.025 for 2022 predictions.

The normal evolution of convergence can be observed in this Figure without any signs of over-fitting. The model is seen to gradually assimilate the useful information contained in the training data. A high rate of drop in RMSE was observed for the first 400 epochs, which was set as the duration of the learning drop period (Table 2). The respective results of the predicted versus actual demand are presented in Figure 17 for the example of January 2022. The values of the selected performance metrics for 2022 are shown in the same Figure: MAPE, μ = 3.56% with σ = 0.42%; nRMSE, μ = 0.049 with σ = 0.006. Compared with the shallow FF ANN model presented in Figures 12 and 13, the mean value of MAPE was a little lower, however, it was higher than the official predictions. However, the standard deviation of MAPE was observably higher than the respective values for both the FF ANN and the official predictions. This may be due to a somewhat higher tendency of the deep networks for data over-fitting, which is not a problem here anyway, as explained above.

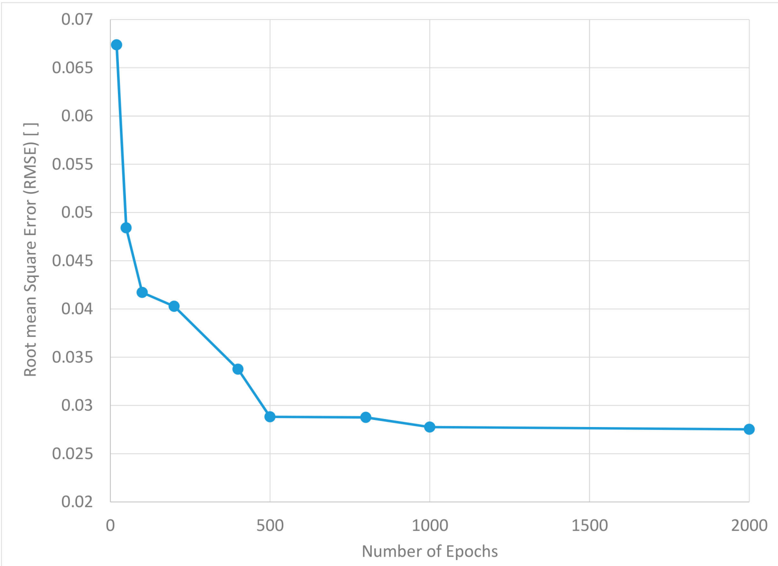

Figure 16. Training progress of deep feed-forward neural network after 20–2000 epochs, as seen by the prediction RMSE for 2022.

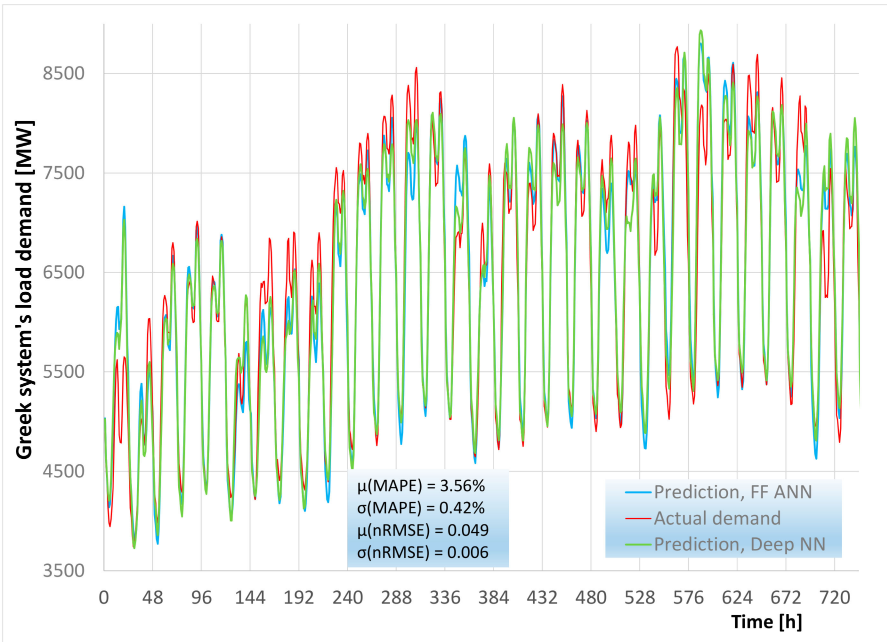

Figure 17. Prediction and validation of system's demand for January 2022, FF-ANN after 81 epochs versus deep NN after 1000 epochs. Modeling error metrics are shown for deep FNN predictions for the whole year 2022.

These values were only a little better than those obtained with the simple FF ANN model, as shown in Figure 12. That is, the additional complexity and CPU time required to run the deep FNN model (a few minutes run on a laptop compared to less than a minute for the FF ANN) did not seem to reward. For comparison, the respective predicted values with the simple FF ANN are drawn in the same diagram. It seems that both types of models incorporated, to a high degree, the information contained in the training dataset. This observation is further supported by the fact that the error metrics of both models are directly comparable to those of the Greek system's operator's forecasting (Figure 1). Moreover, an optical comparison of the two figures points to the similar forecasting behavior of all three models. Similar instances of prediction failures with various types of ANN have been frequently reported by other researchers in different countries [19]. Thus, the cause of specific, short periods of prediction failure should be attributed to the lack of some additional types of training input.

In order to further research this issue, we start with a comparison of the two alternative models' performance against the actual demand for July 2022 (Figure 18). As already reported in Section 2, July and August are more demanding in terms of forecasting, because of the high fluctuations in electricity demand for air conditioning. On the other hand, the models are proven effective in predicting the system's peak demand exceeding 9 GW during 25–28 July. However, both models fail to predict the high levels of demand for the weekend 16–17 July, as shown in detail in Figure 19. The maximum relative error in prediction stays at the same high levels with the official prediction (see Figure 7). In order to better understand the situation and investigate possible ways to improve forecasting accuracy, it is useful to plot, in the same figure, the respective fluctuation of ambient temperatures as recorded by the Psychico weather station during this period.

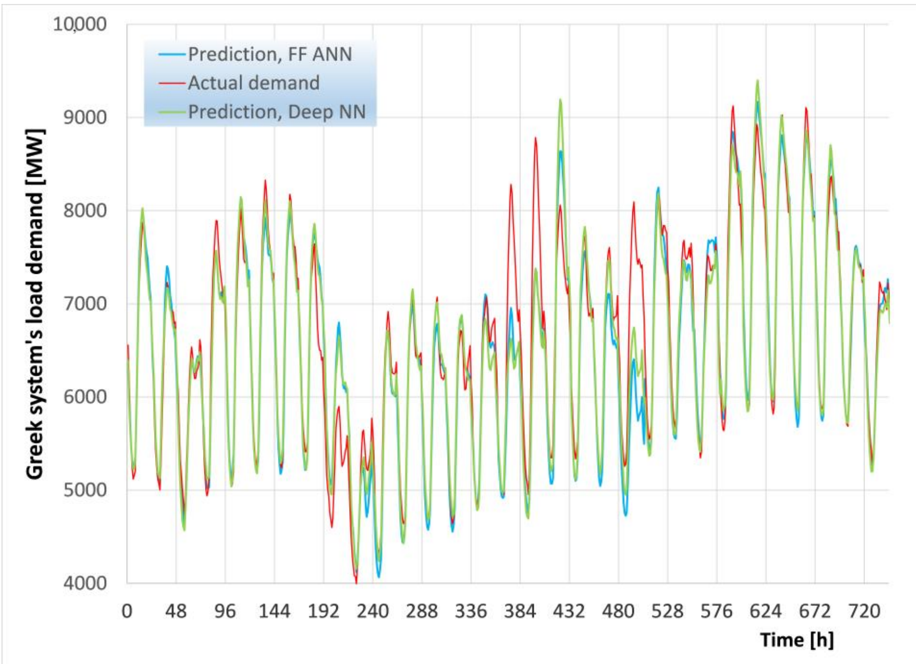

Figure 18. Prediction and validation of system's demand for July 2022, FF-ANN after 81 epochs vs. Deep NN after 1000 epochs.

The temperature during the night before the 16th was seen to stay at about 23–26 °C. Beginning at 06:00 and during the morning hours, we observed a significant increase in ambient temperature, which continued to a maximum of 35 °C between 14:00 and 15:00. Then, a gradual drop in ambient temperature was observed after late afternoon. However, the temperature did not drop to its normal nocturnal levels during the second day and started to ascend earlier Sunday morning. This should place an unexpected burden on the air-conditioning systems and produce a very pronounced morning peak for Saturday and Sunday. The high electricity consumption levels could be attributed to the very high increase of tourists in Greece during this period, which unexpectedly increased the filling rate of hotels and other tourist residences.

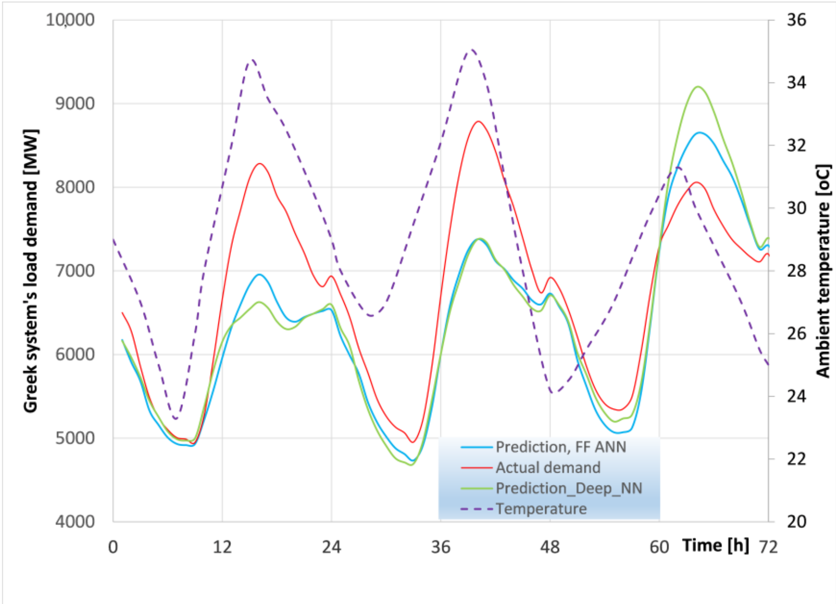

Figure 19. Incident of Saturday 16–Monday 18 July: load prediction failure of both models during a weekend with high temperatures. Maximum relative error is −16.4% for the FF ANN and −19.9% for the deep NN.

A closer look at the comparison curves of Figure 19 reveals further instances of prediction failure. One of these events is 8 July, when a significant over-prediction of load occurred for both models (Figure 20). This should be correlated with the sudden drop in ambient temperatures, shown in the same figure in the example of the Psychico weather station, and a drop in humidity by shifting to NE winds, which suddenly reduced the need for air-conditioning. Both neural networks over-corrected their prediction for the next day, Friday 9 July, which obviously led to an over-prediction failure this time. Another important failure was observed on Wednesday, 20 July, when a sudden increase in ambient temperatures could not be addressed with the required fast response by both neural network models.

A real-world application of the two FF ANN methods described was carried out according to the following procedure. The computer code was run at midnight of each day to predict the 24 h values of load for the next day. The input data for the FF ANN comprise the following variables and sets: (i) Heating degree days (one value predicted daily by the meteorological service for the Psychico meteorological station). (ii) Cooling degree days (one value daily for the Psychico meteorological station). (iii) Time series of the recorded hourly Greek system load values up to midnight. Data uncertainty exists only for the prediction of heating and cooling degree days for the next day, which is equivalent to the day-ahead prediction of the mean daily temperature.

Improvements in the specific aspects of model performance would require a further increase in synergy between the machine learning models and empirical models, incorporating a faster response of the system's demand to weather conditions by means of an improved transfer function with responses on the order of one hour. To this end, it would be helpful to record the system's demand at an increased frequency (once every 15 min), following the example of other European countries [33].

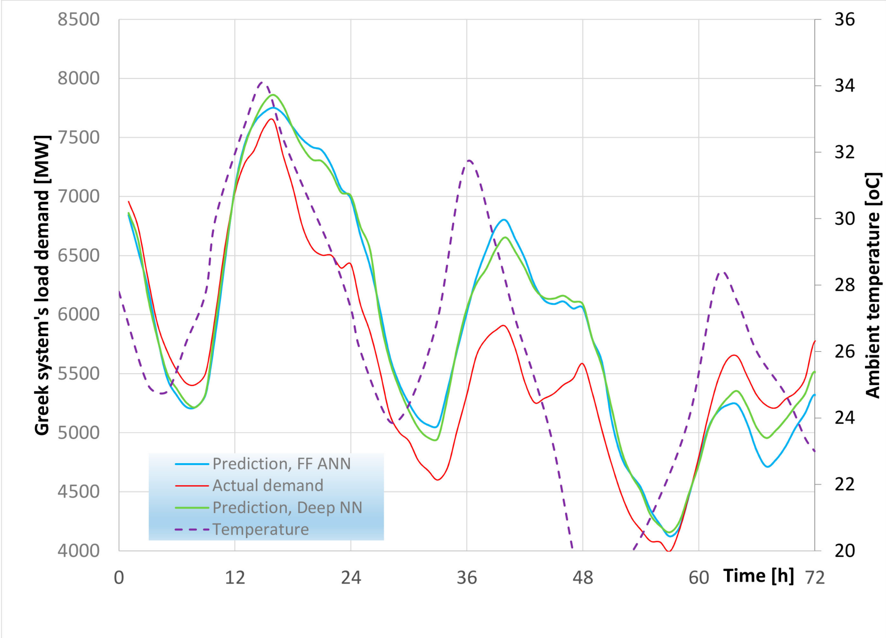

Figure 20. Incident of Thursday 7–Saturday 9 July: load prediction failure of both models during a sudden change to drier weather conditions and ambient temperature drop.

5. Conclusions

This paper applies two standard types of FF ANN models with a novel, simple, and specially designed input training dataset for day-ahead short-term electricity load forecasting in the Greek electricity market. The basic meteorological input comprised the daily heating and cooling degree days from a representative station of Athens. Additional input was the hour of the day, day of the week, a holiday/weekend indicator, and the 24- and 168-hour lagged load of the system. The forecasting capabilities of the two models were compared with the respective predictions of the Greek system's operator's model against the actual data reported in the European platform. The mean value of MAPE of the FF ANN predictions for the 12 months of 2022 was 3.66% (σ = 0.30%) vs. 2.61% (σ = 0.33%) of the official predictions, and the nRMSE was 0.049 (σ = 0.005) vs. 0.036 (σ = 0.005) of the official predictions, respectively. However, our forecasts are true 24-hour-ahead predictions without the noon correction, which is routinely applied by the system's operator. The results suggest that the proposed approach based on a simple and robust FF ANN model, aided by the new design and specific structure of input data, achieves the major goal in 24-hour-ahead prediction. It performs equally well with commercial state-of-the-art tools in day-ahead load forecasting. Specific instances of failure were analyzed, being common to all prediction methodologies and tools examined. They comprise periods with rapid temperature drops with weather changes during summer, which lead to unexpected sudden drops in electricity load for air conditioning. In the future, the effect of incorporating further weather parameters on short-term load forecasting will be examined in the form of air humidity and wind average speed and prevailing direction. Moreover, economic and societal events that may impact grid operation in the form of tourist resident numbers during summer may also be highlighted. Finally, the behavior of Saturday could be distinctively studied and taken care of as a third day typology, instead of just discriminating between workdays and weekends/holidays.

Author Contributions: Conceptualization, G.S. and T.S.; methodology, T.S.; software, G.S.; validation, G.S.; investigation, G.S.; resources, T.S.; data curation, G.S.; writing—original draft preparation, G.S.; writing—review and editing, T.S.; supervision, T.S.; project administration, T.S. All authors have read and agreed to the published version of the manuscript.

Funding: This research received no external funding.

Institutional Review Board Statement: Not applicable.

Informed Consent Statement: Not applicable.

Data Availability Statement: Not applicable.

Conflicts of Interest: The authors declare no conflict of interest.

Nomenclature (Acronyms)

ANN	Artificial Neural Network
BPNN	Back-Propagation Neural Network
CNN	Convolutional Neural Networks
DA	Deterministic Annealing
DB	Dry-Bulb Temperature
DL	Deep Learning
DP	Dew Point Temperature
DSO	Distribution System Operator
ENTSO-E	European Transparency Platform
FF	Feed Forward
GRU	Gated Recurrent Unit
IPTO	Independent Power Transmission Operator
ISO	Independent State Operator
LSTM	Long Short-Term Memory
MAE	Mean Absolute Error
MAPE	Mean Absolute Percentage Error
MBE	Mean Bias Error
ML	Machine Learning
MLP	Multilayer Perceptron
MR	Multiple Regression
MTLF	Medium-Term Load Forecasting
nRMSE	Normalized Root Mean Square Error
PV	Photovoltaic
RBF	Radial Basis Function
RH	Relative Humidity
RMSE	Root Mean Square Error
RNN	Recurrent Neural Network
SDA	Stacked Denoising Autoencoder
SOM	Self-Organizing Map
STLF	Short-Term Load Forecasting
SVM	Support Vector Machine
SVR	Support Vector Regression
TCN	Temporal Convolutional Networks
TSO	Transmission System Operator
WB	Wet Bulb Temperature

References

1. Ahmad, N.; Ghadi, Y.; Adnan, M.; Ali, M. Load Forecasting Techniques for Power System: Research Challenges and Survey. *IEEE Access* **2022**, *10*, 71054–71090. [CrossRef]
2. Sahay, K.B.; Tripathi, M.M. Day ahead hourly load forecast of PJM electricity market and ISO New England market by using artificial neural network. In Proceedings of the 2013 IEEE Innovative Smart Grid Technologies-Asia (ISGT Asia), Bangalore, India, 10–13 November 2013; pp. 1–5.
3. Panapakidis, I.P. Clustering based day-ahead and hour-ahead bus load forecasting models. *Int. J. Electr. Power Energy Syst.* **2016**, *80*, 171–178. [CrossRef]
4. Soliman, S.A.-h.; Al-Kandari, A.M. *Electrical Load Forecasting: Modeling and Model Construction*; Elsevier: Amsterdam, The Netherlands, 2010.
5. Hahn, H.; Meyer-Nieberg, S.; Pickl, S. Electric load forecasting methods: Tools for decision making. *Eur. J. Oper. Res.* **2009**, *199*, 902–907. [CrossRef]

6. Mellit, A.; Pavan, A.M.; Benghanem, M. Least squares support vector machine for short-term prediction of meteorological time series. *Theor. Appl. Climatol.* **2013**, *111*, 297–307. [CrossRef]
7. Mohammadzaheri, M.; Tafreshi, R.; Khan, Z.; Ghodsi, M.; Franchek, M.; Grigoriadis, K. Modelling of petroleum multiphase flow in electrical submersible pumps with shallow artificial neural networks. *Ships Offshore Struct.* **2020**, *15*, 174–183. [CrossRef]
8. Fan, S.; Chen, L. Short-term load forecasting based on an adaptive hybrid method. *IEEE Trans. Power Syst.* **2006**, *21*, 392–401. [CrossRef]
9. Che, J.; Wang, J.; Wang, G. An adaptive fuzzy combination model based on self-organizing map and support vector regression for electric load forecasting. *Energy* **2012**, *37*, 657–664. [CrossRef]
10. Mori, H.; Yuihara, A. Deterministic annealing clustering for ANN-based short-term load forecasting. *IEEE Trans. Power Syst.* **2001**, *16*, 545–551. [CrossRef]
11. Kim, C.-i.; Yu, I.-k.; Song, Y.H. Kohonen neural network and wavelet transform based approach to short-term load forecasting. *Electr. Power Syst. Res.* **2002**, *63*, 169–176. [CrossRef]
12. Martinez Alvarez, F.; Troncoso, A.; Riquelme, J.C.; Aguilar Ruiz, J.S. Energy Time Series Forecasting Based on Pattern Sequence Similarity. *IEEE Trans. Knowl. Data Eng.* **2011**, *23*, 1230–1243. [CrossRef]
13. Cecati, C.; Kolbusz, J.; Różycki, P.; Siano, P.; Wilamowski, B.M. A Novel RBF Training Algorithm for Short-Term Electric Load Forecasting and Comparative Studies. *IEEE Trans. Ind. Electron.* **2015**, *62*, 6519–6529. [CrossRef]
14. Vidal, C.; Haußmann, M.; Barroso, D.; Shamsabadi, P.M.; Biswas, A.; Chemali, E.; Ahmed, R.; Emadi, A. Hybrid Energy Storage System State-of-Charge Estimation Using Artificial Neural Network for Micro-Hybrid Applications. In Proceedings of the 2018 IEEE Transportation Electrification Conference and Expo (ITEC), Long Beach, CA, USA, 13–15 June 2018; pp. 1075–1081.
15. Ozcanli, A.K.; Yaprakdal, F.; Baysal, M. Deep learning methods and applications for electrical power systems: A comprehensive review. *Int. J. Energy Res.* **2020**, *44*, 7136–7157. [CrossRef]
16. Mishra, M.; Nayak, J.; Naik, B.; Abraham, A. Deep learning in electrical utility industry: A comprehensive review of a decade of research. *Eng. Appl. Artif. Intell.* **2020**, *96*, 104000. [CrossRef]
17. Khodayar, M.; Liu, G.; Wang, J.; Khodayar, M.E. Deep learning in power systems research: A review. *CSEE J. Power Energy Syst.* **2021**, *7*, 209–220. [CrossRef]
18. Sun, M.; Zhang, T.; Wang, Y.; Strbac, G.; Kang, C. Using Bayesian Deep Learning to Capture Uncertainty for Residential Net Load Forecasting. *IEEE Trans. Power Syst.* **2020**, *35*, 188–201. [CrossRef]
19. Pavićević, M.; Popović, T. Forecasting Day-Ahead Electricity Metrics with Artificial Neural Networks. *Sensors* **2022**, *22*, 1051. [CrossRef]
20. Pirnia, M.; Elsarague, M.; Beylunioglu, F.C.; Ahmed, M.; Nathwani, J. Impact of COVID-19 on Ontario's electricity market: Load, generation, emissions. *Electr. J.* **2022**, *35*, 107111. [CrossRef]
21. Surakhi, O.; Zaidan, M.A.; Fung, P.L.; Hossein Motlagh, N.; Serhan, S.; AlKhanafseh, M.; Ghoniem, R.M.; Hussein, T. Time-Lag Selection for Time-Series Forecasting Using Neural Network and Heuristic Algorithm. *Electronics* **2021**, *10*, 2518. [CrossRef]
22. Li, Z.; Li, Y.; Liu, Y.; Wang, P.; Lu, R.; Gooi, H.B. Deep Learning Based Densely Connected Network for Load Forecasting. *IEEE Trans. Power Syst.* **2021**, *36*, 2829–2840. [CrossRef]
23. Mir, A.A.; Khan, Z.A.; Altmimi, A.; Badar, M.; Ullah, K.; Imran, M.; Kazmi, S.A.A. Systematic Development of Short-Term Load Forecasting Models for the Electric Power Utilities: The Case of Pakistan. *IEEE Access* **2021**, *9*, 140281–140297. [CrossRef]
24. Guo, Z.; Zhou, K.; Zhang, X.; Yang, S. A deep learning model for short-term power load and probability density forecasting. *Energy* **2018**, *160*, 1186–1200. [CrossRef]
25. Wang, L.; Zhang, Z.; Chen, J. Short-Term Electricity Price Forecasting with Stacked Denoising Autoencoders. *IEEE Trans. Power Syst.* **2017**, *32*, 2673–2681. [CrossRef]
26. Hossen, T.; Plathottam, S.J.; Angamuthu, R.K.; Ranganathan, P.; Salehfar, H. Short-term load forecasting using deep neural networks (DNN). In Proceedings of the 2017 North American Power Symposium (NAPS), Morgantown, WV, USA, 17–19 September 2017; pp. 1–6.
27. Din, G.M.U.; Marnerides, A.K. Short term power load forecasting using Deep Neural Networks. In Proceedings of the 2017 International Conference on Computing, Networking and Communications (ICNC), Santa Clara, CA, USA, 26–29 January 2017; pp. 594–598.
28. Xishuang, D.; Lijun, Q.; Lei, H. Short-term load forecasting in smart grid: A combined CNN and K-means clustering approach. In Proceedings of the 2017 IEEE International Conference on Big Data and Smart Computing (BigComp), Jeju Island, Republic of Korea, 13–16 February 2017; pp. 119–125.
29. Wen, L.; Zhou, K.; Yang, S. Load demand forecasting of residential buildings using a deep learning model. *Electr. Power Syst. Res.* **2020**, *179*, 106073. [CrossRef]
30. Kong, W.; Dong, Z.Y.; Jia, Y.; Hill, D.J.; Xu, Y.; Zhang, Y. Short-Term Residential Load Forecasting Based on LSTM Recurrent Neural Network. *IEEE Trans. Smart Grid* **2019**, *10*, 841–851. [CrossRef]
31. Shi, H.; Xu, M.; Li, R. Deep Learning for Household Load Forecasting—A Novel Pooling Deep RNN. *IEEE Trans. Smart Grid* **2018**, *9*, 5271–5280. [CrossRef]
32. Peng, L.; Lv, S.-X.; Wang, L.; Wang, Z.-Y. Effective electricity load forecasting using enhanced double-reservoir echo state network. *Eng. Appl. Artif. Intell.* **2021**, *99*, 104132. [CrossRef]

33. N.N. Fraunhofer Institute for Systems- und Innovation Research. TEP Energy GmbH and IREES GmbH: FORECAST/eLOAD. Available online: https://www.forecast-model.eu/forecast-en/index.php (accessed on 30 January 2023).
34. IPTO. Independent Power Transmission Operator (Greece): Hourly System Load. Available online: https://www.admie.gr/en (accessed on 30 January 2023).
35. ENTSO-E. Transparency Platform: Central Collection and Publication of Electricity Generation, Transportation and Consumption Data and Information for the Pan-European Market. Available online: https://transparency.entsoe.eu/ (accessed on 30 January 2023).
36. meteo.gr. Athens Weather Stations. Available online: https://www.meteo.gr/cf.cfm?city_id=12 (accessed on 30 January 2023).
37. meteo.gr. Weather Station of Psychico, Athens. Available online: https://penteli.meteo.gr/stations/psychico/ (accessed on 30 January 2023).
38. Xu, R.; Wunsch, D. *Clustering*; Wiley-IEEE Press: Hoboken, NJ, USA, 2008.
39. Hagan, M.T.; Demuth, H.B.; Beale, M.H.; DeJesus, O. *Neural Network Design*, ebook. 2nd ed. 2014. Available online: https://hagan.okstate.edu/NNDesign.pdf (accessed on 30 January 2023).
40. Mohammadzaheri, M.; Chen, L. Intelligent predictive control of a model helicopter's yaw angle. *Asian J. Control.* **2010**, *12*, 667–679. [CrossRef]
41. Tensorflow. An Open Source Machine Learning Framework for Everyone. Available online: https://github.com/tensorflow/tensorflow (accessed on 30 January 2023).
42. Keras. Deep Learning API Written in Python: Layer Activation Functions. Available online: https://keras.io/api/layers/activations/ (accessed on 30 January 2023).
43. Kiartzis, S.J.; Zoumas, C.E.; Bakirtzis, A.G.; Petridis, V. Data pre-processing for short-term load forecasting in an autonomous power system using artificial neural networks. In Proceedings of the Third International Conference on Electronics, Circuits, and Systems, Rhodos, Greece, 13–16 October 1996; Volume 1022, pp. 1021–1024.
44. Roumpakias, E.; Stamatelos, T. Prediction of a Grid-Connected Photovoltaic Park's Output with Artificial Neural Networks Trained by Actual Performance Data. *Appl. Sci.* **2022**, *12*, 6458. [CrossRef]
45. Roumpakias, E.; Stamatelos, T. Health Monitoring and Fault Detection in Photovoltaic Systems in Central Greece Using Artificial Neural Networks. *Appl. Sci.* **2022**, *12*, 2016. [CrossRef]
46. Mohammadzaheri, M.; Ziaiefar, H.; Ghodsi, M.; Emadi, M.; Zarog, M.; Soltani, P.; Bahadur, I. Adaptive Charge Estimation of Piezoelectric Actuators with a Variable Sensing Resistor, an Artificial Intelligence Approach. *Eng. Lett.* **2022**, *30*, 1–8.
47. Shrestha, A.; Mahmood, A. Review of Deep Learning Algorithms and Architectures. *IEEE Access* **2019**, *7*, 53040–53065. [CrossRef]
48. Vidal, C.; Kollmeyer, P.; Naguib, M.; Malysz, P.; Gross, O.; Emadi, A. Robust xEV Battery State-of-Charge Estimator Design Using a Feedforward Deep Neural Network. *SAE Int. J. Adv. Curr. Pract. Mobil.* **2020**, *2*, 2872–2880. [CrossRef]
49. Mouloodi, S.; Rahmanpanah, H.; Gohari, S.; Burvill, C.; Davies, H.M.S. Feedforward backpropagation artificial neural networks for predicting mechanical responses in complex nonlinear structures: A study on a long bone. *J. Mech. Behav. Biomed. Mater.* **2022**, *128*, 105079. [CrossRef]
50. Kingma, D.P.; Ba, J. Adam: A Method for Stochastic Optimization. *arXiv* **2014**, arXiv:1412.6980.